

Title	Size and emission color tuning in the solution phase synthesis of highly luminescent germanium nanocrystals
Authors	Carolan, Darragh;Doyle, Hugh
Publication date	2014-03-21
Original Citation	CAROLAN, D. & DOYLE, H. 2014. Size and emission color tuning in the solution phase synthesis of highly luminescent germanium nanocrystals. Journal of Materials Chemistry C, 2, pp. 3562-3568. doi: 10.1039/C4TC00319E
Type of publication	Article (peer-reviewed)
Link to publisher's version	10.1039/C4TC00319E
Rights	© 2014, the Authors.
Download date	2024-03-29 07:05:23
Item downloaded from	<a href="https://hdl.handle.net/10468/2508">https://hdl.handle.net/10468/2508</a>

## ARTICLE

# Size and Emission Color Tuning in the Solution Phase Synthesis of Highly Luminescent Germanium Nanocrystals

Cite this: DOI: 10.1039/x0xx00000x

Darragh Carolan<sup>a</sup> and Hugh Doyle<sup>a</sup>

Received 00th January 2012,

Accepted 00th January 2012

DOI: 10.1039/x0xx00000x

[www.rsc.org/](http://www.rsc.org/)

**Abstract:** Highly luminescent germanium nanocrystals (NCs) are synthesized at room temperature by hydride reduction of germanium tetrachloride (GeCl<sub>4</sub>) within inverse micelles. Regulation of the Ge NC size is achieved by varying the alkyl chain length of the cationic quaternary ammonium surfactants used to form the inverse micelles. The Ge NCs are chemically passivated with allylamine ligands using a Pt-catalyzed hydrogermylation reaction, minimizing surface oxidation while rendering the NCs dispersible in a range of polar solvents. Transmission electron microscopy shows that the NCs are highly crystalline with well-defined core diameters tuned from 3 to 5 nm. UV-Vis absorbance and photoluminescence (PL) spectroscopy show significant quantum confinement effects, with moderate absorption in the UV spectral range, and a strong, narrow luminescence in the visible with a marked dependency on excitation wavelength. A maximum quantum yield of 20 % is shown for the nanocrystals, and a transition from primarily blue to green emission is observed as the NC diameter increases to 4.5 nm.

## Introduction

In recent years, germanium nanocrystals (Ge NCs) have attracted increasing attention as promising alternatives to II-VI and IV-VI semiconductor materials. As well as being more environmentally friendly than semiconductors containing toxic elements such as Cd, Hg, and Pb, germanium is cheap, biocompatible, electrochemically stable and compatible with existing CMOS processing methods.<sup>1</sup> Germanium is a particularly attractive material for optoelectronic applications as it combines a narrow band gap (0.67 eV) and high carrier mobilities ( $\mu_e = 3900 \text{ cm}^2 \text{ V}^{-1} \text{ s}^{-1}$ ,  $\mu_h = 1900 \text{ cm}^2 \text{ V}^{-1} \text{ s}^{-1}$ ) with a large absorption coefficient (*ca.*  $2 \times 10^5 \text{ cm}^{-1}$ ) and exciton Bohr radius (24 nm).<sup>2-4</sup> As a result, germanium nanostructures are currently being investigated for a variety of potential applications from solar energy conversion and charge storage to hybrid photodetectors and biological imaging.<sup>1,5-7</sup>

An essential prerequisite for many of these optoelectronic applications is the ability to prepare Ge NCs in good yield with narrow size distributions and well characterized surface chemistry, as these define many of their photophysical properties. A number of different synthetic approaches have been reported, including the metathesis reaction of GeCl<sub>4</sub> with Zintl salts,<sup>8-12</sup> reduction of NaGe by ammonium bromide<sup>13</sup> and high temperature decomposition of organogermane precursors.<sup>14-21</sup> Other methods include thermal co-reduction of Ge(II) and amido based precursors,<sup>6,22,23</sup> aqueous phase reduction of GeO<sub>2</sub> powders by NaBH<sub>4</sub>,<sup>24</sup> and other high temperature chemical reduction methods.<sup>25-31</sup> However, disadvantages associated with these methods include

synthetically involved precursor synthesis, long reaction times, high temperatures and pressures, and extensive post synthetic purification procedures.<sup>1,29</sup> As well as the variation in size distribution, morphology and surface chemistries reported above, significant inconsistencies also exist in the photophysical properties of these nanostructures, precluding a detailed understanding of their size-dependent characteristics. One promising approach towards scalable preparation of size monodisperse Ge NCs is the solution phase reduction of germanium halides within inverse micelles at room temperature. This approach was first reported by Wilcoxon *et al.*, who used LiAlH<sub>4</sub> to reduce GeX<sub>4</sub> (X = Cl, Br, I) within inverse micelles at room temperature to form 2–10 nm diameter Ge nanocrystals with hydrogenated surfaces.<sup>32</sup> Veinot and co-workers later produced hydride-terminated Ge NCs with an average diameter of 5 nm via reduction of GeI<sub>4</sub> with LiAlH<sub>4</sub> using cetyltrimethylammonium bromide (CTAB) as a surfactant.<sup>33</sup> Subsequent modification of the NC surface by thermally initiated hydrogermylation resulted in alkyl terminated NCs. Warner and Tilley prepared size monodisperse 5 nm Ge NCs by reducing GeCl<sub>4</sub> within tetraoctylammonium bromide (TOAB) micelles, modifying the surface of the as-synthesized Ge NCs using a Pt-catalyzed hydrogermylation reaction to form allylamine-terminated NCs with covalent Ge-C bonds. This surface modification strategy chemically passivates the nanocrystal surface to prevent oxidation.<sup>34</sup> Tilley and co-workers later examined the formation of Ge NCs using a series of metal hydrides to reduce GeCl<sub>4</sub> within pentaethyleneglycolmonododecyl ether (C<sub>12</sub>E<sub>5</sub>) micelles at room temperature. Stronger reducing agents generally produced

smaller (4.0 - 5.5 nm) particles, but substitution of aluminium hydride reducing agents with borohydrides resulted in much larger and more polydisperse ( $25.0 \pm 15.0$  nm) Ge NCs.<sup>35</sup>

Despite the successes of the microemulsion synthesis approach for preparation of high quality, size monodisperse Ge NCs, the effect of the surfactant structure in determining the size and shape of the resultant Ge NCs has not been examined. In this paper, we report the room-temperature synthesis of size monodisperse amine-terminated Ge NCs within inverse micelles, with well-defined core diameters that may be tuned from 3 to 5 nm. These NCs are readily dispersed in water, acetonitrile, ethanol, chloroform and other polar organic solvents, making them amenable to low cost, solution based device processing. Regulation of the Ge NCs size was achieved by variation of the cationic quaternary ammonium salts used to form the inverse micelles. These water-dispersed Ge NCs exhibit a strong, narrow luminescence with a transition from

primarily blue to green emission as the NC diameter increases from 3.5 to 4.5 nm.

## Results and discussion

Amine-terminated Ge NCs were synthesized by room temperature reduction of germanium tetrachloride by lithium aluminium hydride under an inert atmosphere; see Experimental Section for further details. Figure 1 shows low magnification transmission electron microscope (TEM) images of Ge NCs prepared in the presence of the cationic quaternary ammonium salts tetrabutylammonium bromide (TBAB), tetrahexylammonium bromide (THAB), tetraoctylammonium bromide (TOAB), tetrakis(decyl)ammonium bromide (TKAB), see Figure ES11 in the Electronic Supporting Information for chemical structures of these surfactants.

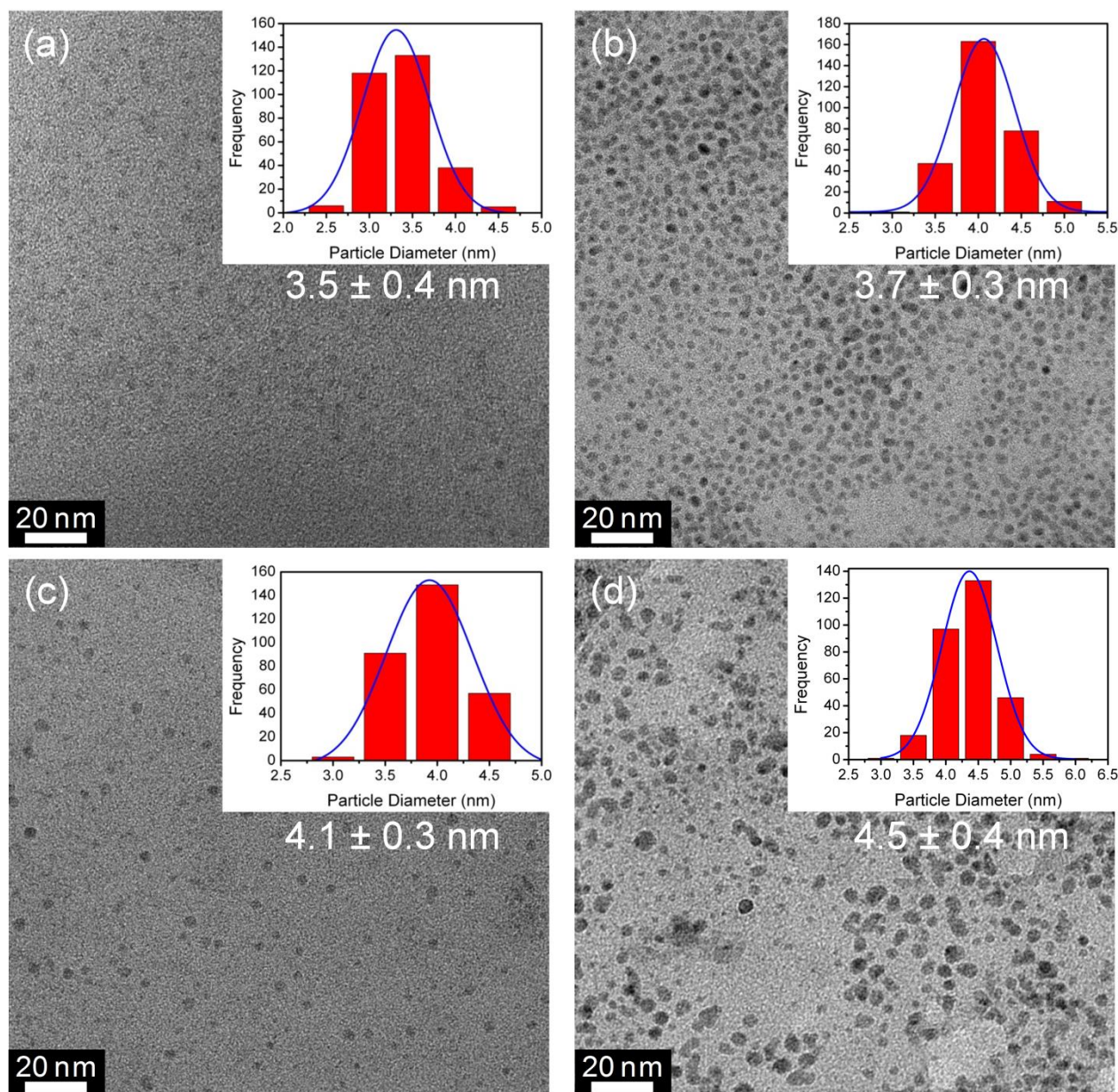


**Fig. 1.** TEM images of Ge NCs synthesized using the various cationic surfactants (a) TBAB, (b) THAB, (c) TOAB and (d) TKAB. Inset: Size histograms of Ge NCs with curves fitted to the data using a Gaussian model.



TEM imaging of Ge NCs synthesized in the presence of TBAB as the surfactant template (Figure 1(a)) show that the Ge NCs are highly size and shape monodisperse, with no evidence of aggregation. Inset in Figure 1(a) is a histogram of NC diameters. Fitting the histogram to a Gaussian model yielded a mean diameter of 3.5 nm, with a standard deviation of 0.4 nm, closely matching the (111) spacing of bulk germanium, emphasizing the highly size monodisperse nature of the NCs. Replacing TBAB with THAB, TOAB or TKAB resulted in an increase in the mean NC diameter to  $3.7 \pm 0.3$  nm,  $4.1 \pm 0.3$  nm and  $4.5 \pm 0.4$  nm respectively, see Figures 1(b)-(d). These TEM imaging results demonstrate that selection of the appropriate surfactant allows a high degree of control over the average NC diameter while maintaining the size monodispersity of the sample. A strong correlation is observed between the alkyl chain length of the surfactant and the Ge NC size, with an average increase in the NC diameter from 3.5 to 4.5 nm as the surfactant side chains are increased from  $C_4$  to  $C_{10}$ .

High-resolution TEM (HR-TEM) imaging was used in conjunction with selective area electron diffraction (SAED) to confirm the crystallinity and establish the crystal phase of the NCs; see Figures 2(a) and (b). HR-TEM imaging (Figure 2(a)) showed that the Ge NCs form a single contiguous crystalline phase, without the presence of packing defects. The lattice fringes shown in Figure 2(a) correspond to a  $d$  spacing of 2.0 Å, matching the (220) spacing reported for the germanium unit cell. SAED patterns of the Ge NCs (Figure 2(b)) showed reflections that could be indexed to Ge diamond cubic (Fd3m) lattice at 2.0 Å (220), 1.7 Å (311), 1.3 Å (331) and 1.2 Å (422), respectively.

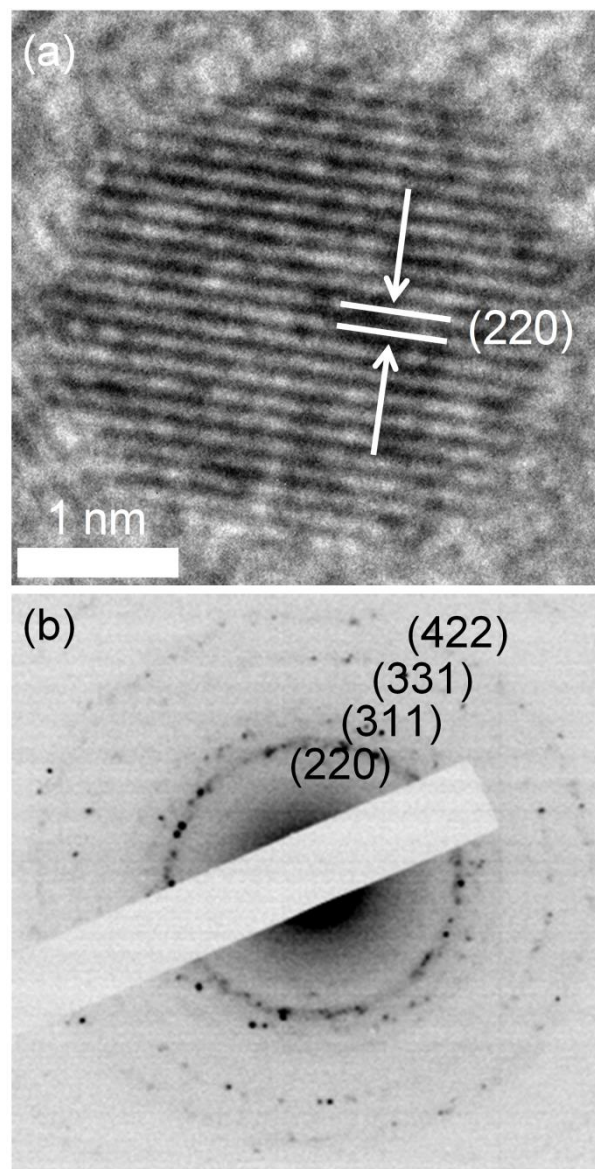


**Fig. 2.** (a) HR-TEM image of an individual Ge NC. (b) SAED pattern of as-synthesized Ge NCs, with the reflections characteristic of crystalline Ge indexed.

The surface chemistry of the quantum dots was characterized by fourier transform infrared spectroscopy (FTIR), see Figure 3. The peaks at 3690 and 3605  $\text{cm}^{-1}$  are assigned to the N-H stretching of the amine, while the band at 1602  $\text{cm}^{-1}$  is attributed to the N-H scissoring mode.<sup>36</sup> The features observed between 3000–2850  $\text{cm}^{-1}$  are attributed to C-H stretching modes.<sup>37</sup> The peaks observed at 1458 and 1260  $\text{cm}^{-1}$  are attributed to scissoring and symmetric bending of the Ge-C bond, respectively. The strong peak at 1098  $\text{cm}^{-1}$  is assigned to the C-N stretching mode of the amine group.<sup>38</sup> The absence of the characteristic  $\text{CH}=\text{CH}_2$  peaks at 900, 1640 and 3080  $\text{cm}^{-1}$ , combined with the formation of the Ge-C bond at 1458 and 1260  $\text{cm}^{-1}$ , indicate covalent attachment of the allylamine ligand to the NC surface. The absence of peaks between 1000–800  $\text{cm}^{-1}$ , previously reported for Ge–O stretching vibrations,<sup>21,23,28</sup> indicates that the germanium nanocrystals are well passivated with minimal surface oxidation.

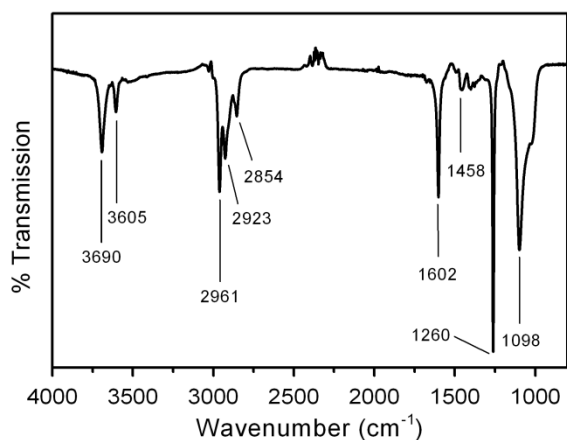


Fig. 3. FTIR spectrum of the allylamine-terminated Ge NCs.

Figure 4, inset shows the UV-Vis absorption spectra of the Ge NCs prepared using the different surfactants. The spectra are very similar, with a strong absorbance in the UV and a tail extending into the visible region, in agreement with previous reports for allylamine-capped semiconductor nanocrystals.<sup>34</sup> While the spectrum of the 3.5 nm NCs is almost featureless, an additional shoulder near 300 nm is observed in the spectra of the 3.7 and 4.1 nm Ge NCs. Increasing the NC diameter to 4.5 nm results in a significant red-shift in the overall spectrum and the emergence of an additional peak centered near 360 nm. Tauc plots of the absorption data showed strong quantum confinement effects within the NCs, with an onset of absorption between 3.1 and 2.8 eV for Ge NCs between 3.5 to 4.1 nm in diameter, while the 4.5 nm NCs had an onset close to 2.5 eV, see Figure 4.

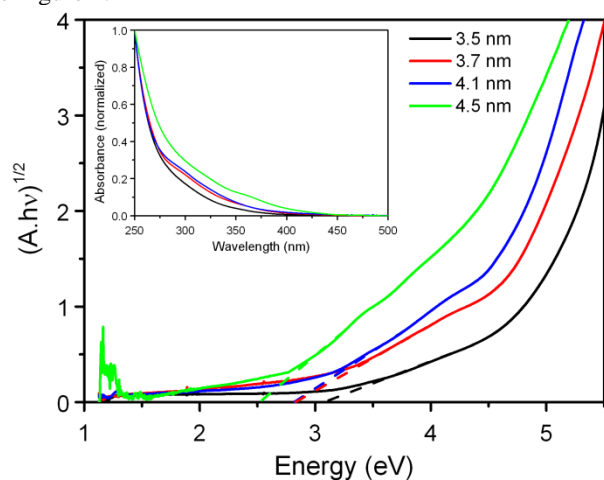


Fig. 4. Tauc plots determined from the absorption data. Inset: Normalized UV-Vis absorption spectra of Ge NCs dispersed in water.

Figure 5(a) shows the normalized PL spectra of aqueous dispersions of the allylamine-capped Ge nanocrystals prepared using the four surfactants. The 3.5 and 3.7 nm diameter NCs exhibited a strong blue emission centered at *ca.* 460 nm (2.7 eV), with a tail extending into the red region of the spectrum. Increasing the NC diameter to 4.1 nm was accompanied by the emergence of a shoulder in the PL spectrum at *ca.* 540 nm (2.3 eV). Further increasing the NC diameter to 4.5 nm resulted in a marked transition from blue to green emission, with complete

suppression of the peak centered at 460 nm, and the emergence of a new peak centered at *ca.* 545 nm with a very narrow full width at half maximum (FWHM) of 50 nm, in agreement with reports for highly size monodisperse green luminescent Ge NCs.<sup>39</sup>

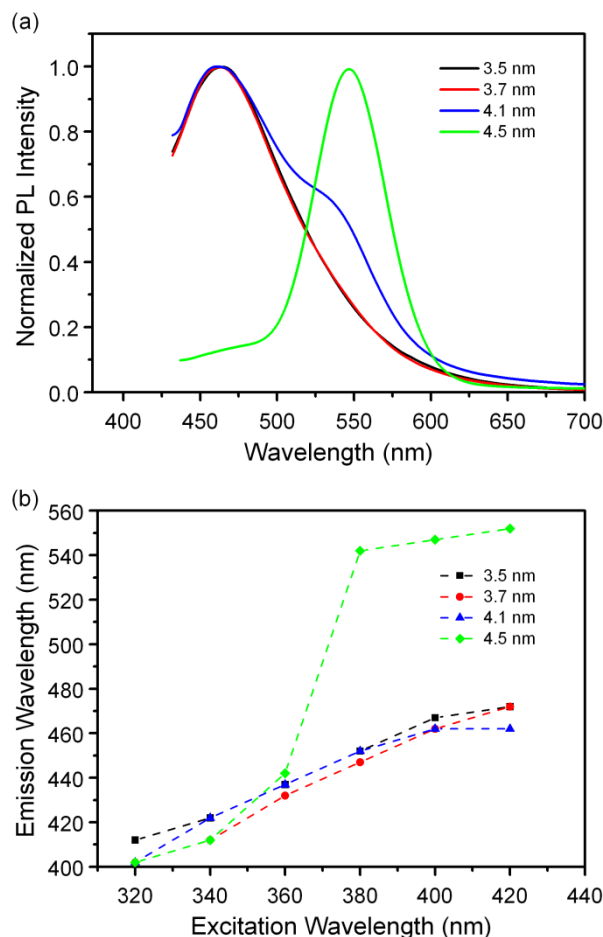


Fig. 5. (a) Photoluminescence spectra of aqueous dispersions of Ge NCs recorded using an excitation wavelength of 400 nm. (b) Wavelength position of the luminescence maximum as a function of excitation wavelength.

All the NC dispersions show a strong dependence between the wavelength position of the PL maximum and the excitation wavelength, see Figure 5(b). For the three smaller Ge NCs, increasing the excitation wavelength from 320 to 420 nm results in a *ca.* 60 nm red shift in the position of the PL maximum. In contrast to this, the largest Ge NCs (4.5 nm) exhibited a marked transition (*ca.* 100 nm) from primarily blue to green emission at excitation wavelengths above 360 nm. The maximum PL intensity for 3.5 to 4.1 nm NCs was observed for 340 nm excitation (3.65 eV), significantly exceeding the energy of the absorption edge (3.1 eV), see Figure 4. A decrease in the relative PL intensity is observed at increasing excitation wavelengths (see Figures ESI2(a)-(b) of the Electronic Supporting Information), in agreement with previous reports. 4.1 nm Ge NCs exhibited similar trends in their photophysical response, with the emergence of an additional shoulder at excitation wavelengths at or above 400 nm, see Figure ESI2(c). The 4.5 nm Ge NCs showed a similar wavelength dependence from 320 to 360 nm for blue emission, with an significantly more intense green emission observed at excitation wavelengths from 380 to 420 nm, see Figure ESI2(d). This

wavelength dependence has previously been attributed to sample polydispersity, with the smaller NCs being selectively excited at shorter wavelengths, and larger NCs at longer wavelengths. However, the narrow size distributions in the Ge NCs reported here preclude this argument, while the transition from blue to green emission with increasing NC diameter indicate that quantum confinement effects play a significant role.

The microscopic origin of the blue-green luminescence observed in organically terminated Group IV nanocrystals remains unresolved. The wide variety of synthetic strategies reported, together with broad particle size distributions, different ligand passivation strategies and varying degrees of surface oxidation have all contributed to the lack of consensus.<sup>1,9,29,33-35</sup> The underlying mechanism is usually described in terms of quantum size effects where the electron-hole pairs are well confined within the nanocrystal core, a surface chemistry model that emphasizes the importance of species at the nanocrystal surface, or a combination of both. The marked size dependency observed in the UV-Vis absorption spectra shown in Figure 4 agrees well with the quantum confinement model. Photoluminescence excitation (PLE) spectra of the Ge NCs recorded at their PL maxima are shown in Figure ESI3 of the Electronic Supporting Information. The three smaller Ge NCs exhibit similar spectra, with two distinct peaks observed at *ca.* 260 and 340 nm, which are most likely due to direct  $\Gamma$ - $\Gamma$  band gap transitions.<sup>32</sup> In contrast, the PLE spectrum of the 4.5 nm Ge NCs shows a single peak centered at 400 nm, close to the onset of absorption determined from the Tauc plots shown in Figure 4, suggesting a lowering of the energies required for exciton generation, consistent with quantum confinement effects within the Ge nanocrystalline core. PL spectra of the Ge NCs dispersed in a variety of polar organic solvents (see Figure ESI4 of the Electronic Supporting Information) show broadly similar PL spectra and excitation wavelength dependency, though the shifting in the position of the PL maxima indicates some involvement of NC surface species.

Photoluminescence quantum yields (QY) were determined using 9, 10-diphenylanthracene and fluorescein as reference emitters for blue and green emissive NCs, see Experimental Section for further details. Figure 6(a) shows the integrated PL intensity (340 nm excitation) of dilute dispersions of the blue emitting Ge NCs (3.5, 3.7 & 4.1 nm diameter) compared with solutions of 9, 10-diphenylanthracene recorded under identical excitation conditions. The quantum yields of the 3.5 and 3.7 nm Ge NCs were 19 and 20 % respectively, comparable to QY values reported in the literature, which range from 11 to 17 %.<sup>34,35,39,40</sup> The 4.1 nm Ge NCs exhibit a lower QY value of 12 %. Figure 6(b) shows the integrated PL intensity (400 nm excitation) of dilute dispersions of the green emitting 4.5 nm Ge NCs compared with aqueous solutions of fluorescein. The quantum yield of the Ge NCs was found to be 8 % at the optimal excitation wavelength of 400 nm, again in good comparison with the literature.

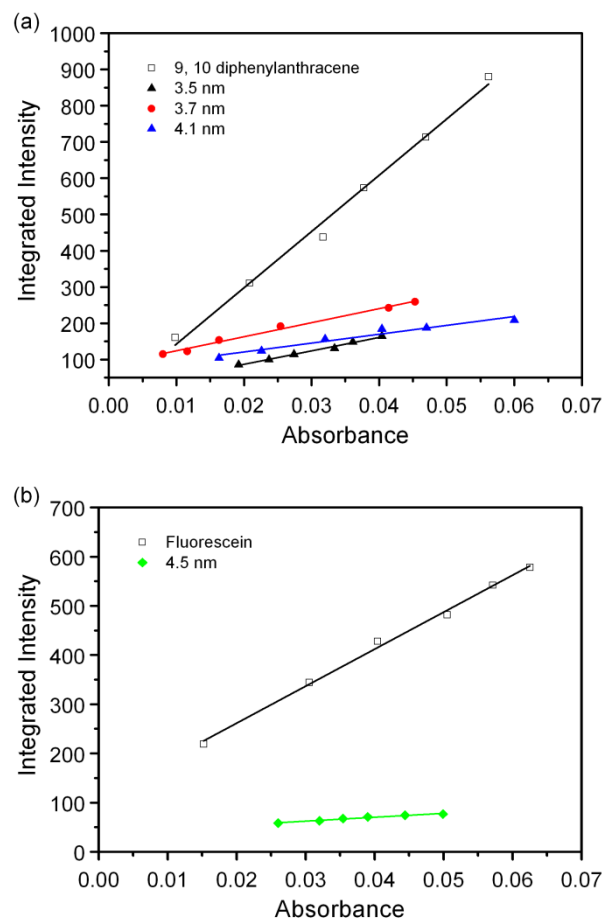


**Fig. 6.** (a) Integrated PL intensity versus absorbance for dilute dispersions of blue emitting Ge NCs and 9, 10-diphenylanthracene. (b) Integrated PL intensity versus absorbance for dilute dispersions of green emitting Ge NCs and fluorescein.

## Conclusions

Highly luminescent germanium nanocrystals have been synthesized using a room temperature, solution phase synthesis method by hydride reduction of germanium tetrachloride ( $\text{GeCl}_4$ ) within inverse micelles. Regulation of the Ge NC diameter from 3.5 to 4.5 nm is achieved by selection of the alkyl chain length of the cationic quaternary ammonium surfactants used to form the micelles. TEM imaging confirmed that the NCs were highly crystalline with narrow size distributions, while the crystal structure of Ge was confirmed by SAED. FTIR confirmed that the surface of water-dispersed nanocrystals possessed covalently bound allylamine ligands, with minimal surface oxidation. UV-Vis absorbance and photoluminescence spectroscopy show significant quantum confinement effects, with moderate absorption in the UV spectral range, and a strong luminescence in the visible with a marked dependency on excitation wavelength. These NCs may also be readily dispersed in acetonitrile, ethanol, chloroform and other polar organic solvents, making them amenable to low cost, solution based device processing. A maximum photoluminescence quantum yield of 20 % was observed for the nanocrystals, while a transition from primarily blue to green emission was observed as the NC diameter was increased to 4.5 nm.

## Experimental Section

### Chemicals.

Tetrabutylammonium bromide (98 %), tetrahexylammonium bromide (99 %), tetraoctylammonium bromide (98 %), tetrakis(decyl)ammonium bromide (98 %), 9, 10-diphenylanthracene (97 %), fluorescein (for fluorescence), cyclohexane (CHROMASOLV Plus, for HPLC,  $\geq 99.9$  %), NaOH (BioUltra, for luminescence,  $\geq 98.0$  %), sulfuric acid (95-97 %) and hydrogen peroxide (30% v/v) were purchased from Sigma Aldrich Ltd. and stored under ambient atmosphere. Germanium tetrachloride (99.99 %), chloroplatinic acid ( $\geq 99.9$  %), lithium aluminium hydride (1M in THF), allylamine ( $\geq 99$  %), toluene (99.8 %, anhydrous), methanol (99.8 %, anhydrous) and propan-2-ol (99.5 %, anhydrous) were purchased from Sigma Aldrich Ltd. and stored under inert atmosphere before use. All materials and solvents were used as received.

### Synthesis and Purification.

All synthetic manipulations were carried out in an inert atmosphere glove box. All glassware used was cleaned by soaking in a base bath overnight, followed by immersion in piranha solution (3:1 concentrated sulfuric acid: 30 % hydrogen peroxide) for 20 minutes. *CAUTION: Piranha solution is a strong oxidizing agent and should be handled with extreme care.* In a typical preparation, 2.74 mmol of the surfactant was dissolved in 60 mL toluene in a 2-neck round bottomed flask with continuous stirring. 0.1 mL (0.876 mmol)  $\text{GeCl}_4$  was then added to the solution and left to stir for 30 min. Ge NCs were formed by the drop wise addition of 2 mL of  $\text{LiAlH}_4$  over a period of 2 minutes. *CAUTION: Germane gas, which is pyrophoric and highly toxic, may be evolved at this stage of the reaction and care should be taken to prevent exposure to air.*<sup>41</sup> The solution was then left to stir for 2.5 h. The excess reducing agent was then quenched with the addition of 20 mL methanol. At this stage of the reaction the Ge NCs are terminated by hydrogen and encapsulated within the inverse micelle.

Chemically passivated nanocrystals were formed by modifying the germanium-hydrogen bonds at the surface via the addition of 0.5 mL of 0.1 M chloroplatinic acid in propan-2-ol as a catalyst, followed by 2 mL of allylamine. After stirring for 2.5 h, the Ge NCs were removed from the glove box and the organic solvent removed by rotary evaporation. The resulting brown dry powder (consisting of surfactant and Ge NCs) was then re-dispersed in 40 mL deionized water (18.2 M $\Omega$  cm) and sonicated for 20 min. The solution was first filtered using filter paper and then PTFE membrane filters (Acrodisc, 0.45  $\mu\text{m}$ ) to remove the surfactant. Amine-terminated Ge NCs remain in the water phase. The Ge NCs were further purified by chromatography. The solution was concentrated down to ca. 1.5 mL and loaded into the column ( $\phi$  1 cm, 47.0 cm). Sephadex gel LH-20 was used as the stationary phase: fractions of ca. 3 mL were collected at a drop rate of approximately 1 drop every 25 seconds. The fractions were then combined and concentrated down to ca. 5 mL.

### Characterization.

UV-Vis absorption spectra were recorded using a Shimadzu UV PC-2401 spectrophotometer equipped with a 60 mm integrating sphere (ISR-240A, Shimadzu). Spectra were recorded at room temperature using a quartz cuvette (1 cm) and corrected for the solvent absorption. Photoluminescence spectra

were recorded using an Agilent Cary Eclipse spectrophotometer. Quantum yields were measured using the comparative method described by Williams *et al.*<sup>42</sup> Dilute solutions of the Ge NCs in water were prepared with optical densities between 0.01 - 0.1 and compared against solutions of the reference emitters 9, 10-diphenylanthracene in cyclohexane and fluorescein in 0.1 M NaOH with similar optical densities. PL spectra of Ge NCs and reference solutions were acquired using an appropriate excitation wavelength, and the total PL intensity integrated over a suitable range for each set of NCs and reference emitters. FTIR spectra were recorded on a Perkin Elmer Two spectrometer. Spectra were recorded on aliquots of Ge NCs dispersed in chloroform in a liquid cell with  $\text{CaF}_2$  plates.

Transmission electron microscopy images and selective area electron diffraction patterns were acquired using a high-resolution JEOL 2100 electron microscope, equipped with a  $\text{LaB}_6$  thermionic emission filament and Gatan DualVision 600 Charge-Coupled Device (CCD), operating at an accelerating voltage of 200 keV. TEM samples were prepared by depositing a 40  $\mu\text{L}$  aliquot of the Ge NC dispersion onto a holey carbon-coated copper grid (300 mesh, #S147-3, Agar Scientific), which was allowed to evaporate under ambient conditions. Data for size distribution histograms was acquired by analysis of TEM images of exactly 300 NCs located at different regions of the grid. NC diameter was determined by manual inspection of the digital images; in the case of anisotropic structures, the diameter was determined using the longest axis.

## Acknowledgements

This work was supported by the European Commission under the FP7 Projects SNAPSUN (grant agreement n $^\circ$  246310) and CommonSense (grant agreement n $^\circ$  261809) and the Irish Higher Education Authority under the PRTL programs (Cycle 3 “Nanoscience” and Cycle 4 “INSPIRE”).

## Notes and references

<sup>a</sup> Tyndall National Institute, University College Cork, Lee Maltings, Cork, Ireland.

Email: hugh.doyle@tyndall.ie

Electronic Supplementary Information (ESI) available: [Chemical structures of the surfactant molecules, photoluminescence spectra, photoluminescence excitation spectra and photoluminescence spectra in various solvents]. See DOI: 10.1039/b000000x/

1. D. D. Vaughn II and R. E. Schaak, *Chem. Soc. Rev.*, 2013, **42**, 2861.
2. R. Pillarisetty, *Nature*, 2011, **479**, 324.
3. Y. Kamata, *Mater. Today*, 2008, **11**, 30.
4. M. Seino, E. J. Henderson, D. P. Puzzo, N. Kadota and G. A. Ozin, *J. Mater. Chem.*, 2011, **21**, 15895.
5. D.-J. Xue, J.-J. Wang, Y.-Q. Wang, S. Xin, Y.-G. Guo and L.-J. Wan, *Adv. Mater.*, 2011, **23**, 3704.
6. T. N. Lambert, N. L. Andrews, H. Gerung, T. J. Boyle, J. M. Oliver, B. S. Wilson and S. M. Han, *Small*, 2007, **3**, 691.
7. Z. C. Holman, C.-Y. Liu and U. R. Kortshagen, *Nano Lett.*, 2010, **10**, 2661.
8. B. R. Taylor, S. M. Kauzlarich, H. W. H. Lee and G. R. Delgado, *Chem. Mater.*, 1998, **10**, 22.

9. B. R. Taylor, S. M. Kauzlarich, G. R. Delgado and H. W. H. Lee, *Chem. Mater.*, 1999, **11**, 2493.
10. B. R. Taylor, G. A. Fox, L. J. Hope-Weeks, R. S. Maxwell, S. M. Kauzlarich and H. W. H. Lee, *Mater. Sci. Eng., B*, 2002, **96**, 90.
11. R. S. Tanke, S. M. Kauzlarich, T. E. Patten, K. A. Pettigrew, D. L. Murphy, M. E. Thompson and H. W. H. Lee, *Chem. Mater.*, 2003, **15**, 1682.
12. A. J. Pugsley, C. L. Bull, A. Sella, G. Sankar and P. F. McMillan, *J. Solid. State. Chem.*, 2011, **184**, 2345.
13. X. Ma, F. Wu and S. M. Kauzlarich, *J. Solid. State. Chem.*, 2008, **181**, 1628.
14. X. M. Lu, K. J. Ziegler, A. Ghezelbash, K. P. Johnston and B. A. Korgel, *Nano Lett.*, 2004, **4**, 969.
15. X. M. Lu, B. A. Korgel and K. P. Johnston, *Nanotechnology*, 2005, **16**, S389.
16. D. Gerion, N. Zaitseva, C. Saw, M. F. Casula, S. Fakra, T. Van Buuren and G. Galli, *Nano Lett.*, 2004, **4**, 597.
17. N. Zaitseva, Z. R. Dai, C. D. Grant, J. Harper and C. Saw, *Chem. Mater.*, 2007, **19**, 5174.
18. E. J. Henderson, C. M. Hessel and J. G. C. Veinot, *J. Am. Chem. Soc.*, 2008, **130**, 3624.
19. E. J. Henderson, C. M. Hessel, R. G. Cavell and J. G. C. Veinot, *Chem. Mater.*, 2010, **22**, 2653.
20. M. Hoffman and J. G. C. Veinot, *Chem. Mater.*, 2012, **24**, 1283.
21. E. J. Henderson, M. Seino, D. P. Puzzo and G. A. Ozin, *ACS Nano*, 2010, **4**, 7683.
22. T. J. Boyle, L. J. Tribby, L. A. M. Ottley and S. M. Han, *Eur. J. Inorg. Chem.*, 2009, **2009**, 5550.
23. H. Gerung, S. D. Bunge, T. J. Boyle, C. J. Brinker and S. M. Han, *Chem. Commun.*, 2005, 1914.
24. J. Wu, Y. Sun, R. Zou, G. Song, Z. Chen, C. Wang and J. Hu, *CrystEngComm*, 2011, **13**, 3674.
25. X. M. Lu, B. A. Korgel and K. P. Johnston, *Chem. Mater.*, 2005, **17**, 6479.
26. D. A. Ruddy, J. C. Johnson, E. R. Smith and N. R. Neale, *ACS Nano*, 2010, **4**, 7459.
27. S. C. Codoluto, W. J. Baumgardner and T. Hanrath, *CrystEngComm*, 2010, **12**, 2903.
28. D. C. Lee, J. M. Pietryga, I. Robel, D. J. Werder, R. D. Schaller and V. I. Klimov, *J. Am. Chem. Soc.*, 2009, **131**, 3436.
29. E. Muthuswamy, A. S. Iskandar, M. M. Amador and S. M. Kauzlarich, *Chem. Mater.*, 2012, **25**, 1416.
30. W. Z. Wang, B. Poudel, J. Y. Huang, D. Z. Wang, S. Kunwar and Z. F. Ren, *Nanotechnology*, 2005, **16**, 1126.
31. D. D. Vaughn, II, J. F. Bondi and R. E. Schaak, *Chem. Mater.*, 2010, **22**, 6103.
32. J. P. Wilcoxon, P. P. Provencio and G. A. Samara, *Phys. Rev. B*, 2001, **64**, 035417.
33. E. Fok, M. L. Shih, A. Meldrum and J. G. C. Veinot, *Chem. Commun.*, 2004, 386.
34. J. H. Warner and R. D. Tilley, *Nanotechnology*, 2006, **17**, 3745.
35. S. Prabakar, A. Shiohara, S. Hanada, K. Fujioka, K. Yamamoto and R. D. Tilley, *Chem. Mater.*, 2010, **22**, 482.
36. J. H. Ahire, Q. Wang, P. R. Coxon, G. Malhotra, R. Brydson, R. Chen and Y. Chao, *ACS Appl. Mater. Interfaces*, 2012, **4**, 3285.
37. R. M. Silverstein, G. C. Bassler and T. C. Morrill, *Spectrometric identification of organic compounds*, Wiley, New York, 1991.
38. G. Socrates, *Infrared characteristic group frequencies*, Wiley, Chichester, 1980.
39. B. Ghosh, Y. Sakka and N. Shirahata, *J. Mater. Chem. A*, 2013, **1**, 3747.
40. N. Shirahata, D. Hirakawa, Y. Masuda and Y. Sakka, *Langmuir*, 2012, **29**, 7401.
41. J. P. Wilcoxon, P. P. Provencio and G. A. Samara, *Phys. Rev. B*, 2007, **76**, 199904.
42. A. T. R. Williams, S. A. Winfield and J. N. Miller, *Analyst*, 1983, **108**, 1067.